Extremely High Upper Critical Magnetic Field of the Noncentrosymmetric Heavy Fermion Superconductor $CeRhSi_3$

N. Kimura, K. Ito, and H. Aoki
Graduate School of Science, Tohoku University, Sendai, Miyagi 980-8578, Japan

S. Uji and T. Terashima
National Institute for Materials Science, Tsukuba, Ibaraki 305-0003, Japan
(Received 13 September 2006; published 7 May 2007)

We report an extremely high upper critical field B_{c2} in the noncentrosymmetric heavy fermion superconductor $CeRhSi_3$ for a magnetic field B along the tetragonal c axis. $B_{c2}(T=0)$ possibly reaching 30 T is much higher than $B_{c2}(0) = 7$ T for $B \perp c$ and greatly exceeds the paramagnetic limiting field. The strong anisotropy of $B_{c2}(0)$ with extremely high $B_{c2}(0)$ for $B \parallel c$ is qualitatively explained by the paramagnetic pair-breaking mechanism specific to the noncentrosymmetric superconductor. However, an unusual $B_{c2}(T)$ curve with a positive curvature for $B \parallel c$ cannot be explained satisfactorily by conventional orbital pair-breaking models.

DOI: 10.1103/PhysRevLett.98.197001 PACS numbers: 74.70.Tx, 74.20.Rp, 74.25.Dw, 74.62.Fj

A superconducting state will be destroyed by the application of a sufficiently strong magnetic field to the superconductor (SC). The magnetic field gives rise to spin polarization due to the Zeeman effect and to cyclotron motion due to the Lorentz force, and then they break apart the Cooper pairs. These depairing mechanisms are called the paramagnetic and orbital pair-breaking effects, respectively. The influence of the former effect depends on the symmetry of the Cooper pairs. It breaks apart the singlet (antiparallel spin) pair but not the triplet (parallel spin) pair. On the other hand, the influence of the latter effect is thought to be independent of the pairing symmetry.

In noncentrosymmetric (NCS) SCs, the spin-orbit interaction with broken inversion symmetry forbids the usual classification of Cooper pairs. Instead, a new pairing symmetry, i.e., a mixed parity state, is expected to be realized [1]. Some theoretical considerations predict modification of the paramagnetic pair-breaking effect [1–4] and a helical-vortex state which reduces the pair-breaking effect [5]. The first NCS heavy fermion (HF) SC $CePt_3Si$ is reported to have an upper critical field $B_{c2}(T=0)$ of 5 T, which exceeds the paramagnetic limiting field of 1 T [6]. The observation of high $B_{c2}(0)$ is explained in terms of these characteristic effects of NCS SCs.

We have discovered a second Ce-based NCS HF SC $CeRhSi_3$ and have observed a relatively high $B_{c2}(0)$ of 7 T for fields along the tetragonal basal plane ($B \parallel a$) [7]. In this Letter, we report a much higher $B_{c2}(0)$, possibly reaching 30 T, for a field along the c axis in $CeRhSi_3$. The extremely high $B_{c2}(0)$ exceeds not only the paramagnetic limiting field but also the orbital limiting one estimated on the basis of the BCS model.

Single crystals of $CeRhSi_3$ were obtained by the same method as in the previous Letter [7]. The residual resistivity and its ratio with current j along the c axis were 0.41 $\mu\Omega$ cm and 240, respectively. These values are comparable to those previously used [7], guaranteeing a clean-limit SC. The setup of the pressure cell and the methods of the resistivity and susceptibility measurements were also the same as those in the previous Letter [7].

The resistivity ρ as a function of T for $j \parallel c$ under several pressures (P) is shown in Fig. 1(a). The resistive drop due to the superconductivity emerges at ambient P, but it is not completed at the lowest T of 20 mK. In the ac-susceptibility measurements, the magnetic shielding starts approximately at the midpoint temperature of the resistive drop. Therefore, we define the temperature at the midpoint as the superconducting transition temperature T_c. With increasing P, T_c increases, and the resistive drop becomes sharper. Perfect shielding is observed in the ac-susceptibility measurements above 15 kbar. T_c reaches a maximum of about 1.1 K at 26 kbar. With further application of P, T_c decreases slightly, and the resistive drop broadens again. The antiferromagnetic ordering temperature T_N [8] increases with increasing pressure, then turns to decrease at 8 kbar, and disappears above 24 kbar. The P dependences of T_N and T_c are shown in Fig. 1(b). Since the superconductivity masks the resistivity anomalies observed at T_N, the critical pressure where the antiferromagnetism vanishes at 0 K is not clear; however, we suppose that it is about 26 kbar.

The resistivity has T^2 dependence below T_N for $P \leq$ 24 kbar. The coefficient A of the T^2 term is almost constant or increases slightly as shown in Fig. 1(c). According to the Kadowaki-Woods relation [9], this suggests that the specific heat coefficient $\gamma = 120$ mJ/mol K^2 at ambient P [8] should be unchanged or should increase slightly up to 24 kbar. For $P > 24$ kbar, the resistivity has T-linear dependence. For $j \parallel a$, the T^2 dependence also changes to the T-linear one and the A of the T^2 term does not have strong P dependence [7].

The resistivity as a function of T for several magnetic fields at 29 kbar is shown in Fig. 2(a). Figure 2(b) shows the resultant field dependence of T_c, namely, the B_{c2}-T

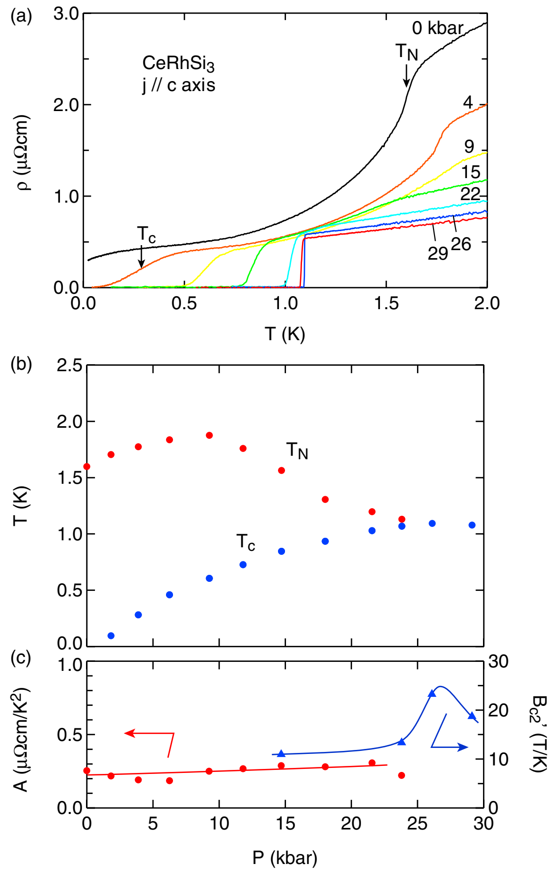

FIG. 1 (color online). (a) Electrical resistivity ρ of $CeRhSi_3$ as a function of T for $0 < P \leq 29$ kbar with $j \parallel c$. (b) T-P phase diagram of $CeRhSi_3$. T_N is taken as the temperature where the resistivity rapidly changes in slope, namely, the inflection point, while the superconducting transition temperature T_c is taken as the midpoint of the resistive drop. (c) Coefficient A of the T^2 term in ρ and the initial slope of the superconducting B_{c2}-T phase diagram as a function of P.

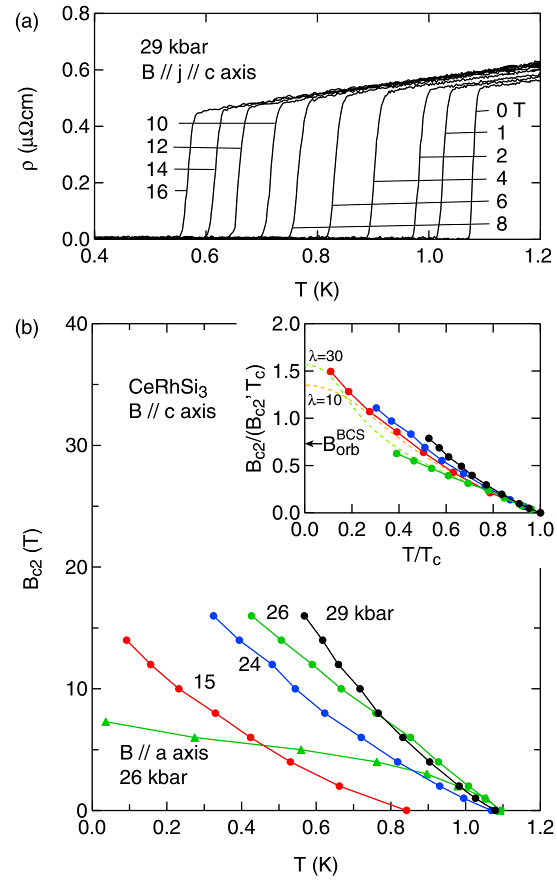

FIG. 2 (color online). (a) Resistivity curves for $B \parallel c$ from 0 to 16 T at 29 kbar. (b) B_{c2}-T phase diagrams for $B \parallel c$ at $P = 15$, 24, 26, and 29 kbar. Inset: $B_{c2}(T)$ curves for the $B \parallel c$ normalized by the initial slope. The arrow indicates the orbital limit $B_{orb}^{BCS} = 0.73 B'_{c2} T_c$ (see text). The dashed curves are theoretical predictions based on the strong-coupling model using the coupling strength parameter $\lambda = 10$ and 30 [20].

phase diagram, compiled from Fig. 2(a). We obtain approximately the same phase diagram constructed from the onset of the magnetic shielding in the ac susceptibility. $B_{c2}(T)$ at 29 kbar reaches 16 T at the temperature $T \approx 0.5 T_c$ and at the lower temperatures exceeds the highest field of 16 T available in our laboratory [10]. The $B_{c2}(T)$ curves at 15, 24, and 29 kbar keep positive curvatures ($d^2 B_{c2}/dT^2 > 0$) down to at least 0.1, 0.3, and $0.5 T_c$, respectively. The $B_{c2}(T)$ curve at 26 kbar is approximately linear. Although T_c for zero field at 29 kbar is slightly smaller than that at 26 kbar, B_{c2} becomes larger than that at 26 kbar at low temperatures.

The initial slope of the upper critical field $B'_{c2} \equiv -(dB_{c2}/dT)|_{T=T_c}$ strongly depends on the applied pressure and seems to have a maximum of 23 T/K at 26 kbar as seen in Fig. 1(c). The maximum value is comparable to that of the other HF SC $CeCu_2Si_2$ ($B'_{c2} = 23$ T/K) with a large γ of 1 J/mol K^2 [11]. The P dependence of A and B'_{c2} suggests a large mass enhancement, probably due to the magnetic fluctuation arising only in the vicinity of the critical pressure, whereas the superconductivity appears in a much wider pressure region: We note that superconductivity is achieved in the pressure region where $dT_N/dP > 0$. These properties are in contrast to those of other pressure-induced HF SCs, in which the appearance of superconductivity is accompanied by strong mass enhancement [12].

One may conjecture that the value of $B_{c2}(0)$ at high pressures exceeds at least 20 T. However, it seems difficult to determine without ambiguity because the $B_{c2}(T)$ curve is significantly different from that predicted by the well-known model [13]. To estimate $B_{c2}(0)$ experimentally without using any theoretical model, we plot $B_{c2}(T)$ normalized by the initial slope, as seen in the inset in Fig. 2(b). Since the form of the curve for 15 kbar has been determined in a wider temperature range, we compare the other curves with that for 15 kbar. The normalized curves for 24 and 29 kbar are similar in nature, although they deviate upward from that for 15 kbar with decreasing T/T_c. Assuming that those curves approximately correspond to that for 15 kbar at low temperatures, we would expect

$B_{c2}/(B'_{c2}T_c)$ to reach at least 1.5 for $T \to 0$, which corresponds to $B_{c2}(0) \approx 22$ and 30 T for 24 and 29 kbar, respectively. The curve for 26 kbar seems to differ in shape from the others. Therefore, we cannot estimate $B_{c2}(0)$ from a comparison with the curve for 15 kbar. Instead, we extrapolate $B_{c2}(0)$ from a linear extension of the data to $T = 0$. We obtain $B_{c2}(0) \approx 26$ T for 26 kbar.

The magnetic phase diagram of the superconductivity in $CeRhSi_3$ is strongly anisotropic, unlike the almost isotropic phase diagram for that in $CePt_3Si$ [14]. $B_{c2}(0)$ and its P dependence for $B \parallel a$ are quite different from those for $B \parallel c$, as seen in Fig. 2(b). $B_{c2}(T)$ for $B \parallel a$ at 26 kbar has a steep initial slope of $B'_{c2} = 27$ T/K as large as that for $B \parallel c$, although $B_{c2}(0)$ of 7 T is quite different from that for $B \parallel c$. The concave structure of the $B_{c2}(T)$ curve observed at 16 kbar [7] becomes less obvious at 26 kbar. $B_{c2}(0)$ is almost independent of P from 16 to 29 kbar, whereas B'_{c2} has a similar P dependence to that for $B \parallel c$. The fact that $B_{c2}(0)$ is independent of B'_{c2} suggests the existence of the paramagnetic pair-breaking effect which is predominant over the orbital one.

The $B_{c2}(0)$-T_c plots for $CeRhSi_3$ and known HF SCs are shown in Fig. 3 [6,11,14–17]. For $CeRhSi_3$, we plot the estimated value of $B_{c2}(0) = 30$ T at 29 kbar. $B_{c2}(0)$ should be larger than 17.5 T [10]. In general, the magnitude of $B_{c2}(0)$ is restricted by both the paramagnetic limiting field B_P and the orbital limiting field B_{orb}. In the BCS model (for a singlet-pairing SC), B_P is given by $B_P^{\mathrm{BCS}} = \sqrt{2}\Delta/(g\mu_B) = 1.86T_c$, where Δ, g, and μ_B are the superconducting gap, gyromagnetic ratio, and Bohr magneton, respectively [18]. The B_P^{BCS} relation is given by the dashed line in Fig. 3. On the other hand, B_{orb} is expressed by $B_{\mathrm{orb}} = \Phi_0/(2\pi\xi_0^2)$, where Φ_0 is the quantum fluxoid and ξ_0 is the superconducting coherence length. If we assume the BCS model (weak-coupling limit), it can be expressed using the initial slope, namely, $B_{\mathrm{orb}}^{\mathrm{BCS}}(0) = 0.73B'_{c2}T_c$ for the clean limit [13].

One can see that some singlet-pairing SCs are situated above the B_P^{BCS} line, although their $B_{c2}(0)$ must not exceed B_P^{BCS}, in general. Two causes have been proposed so far. One is a reduction of the g factor found in $CeCoIn_5$ ($g = 0.63$ for $B \parallel a$) [19] and URu_2Si_2 ($g = 0.23$ for $B \parallel a$) [16]. The other is the strong-coupling effect, which could enhance B_P and successfully explain the large $B_{c2}(0)$ of UBe_{13} [20]. For a NCS SC, two additional mechanisms, i.e., reduced paramagnetic pair breaking [1–4] and the helical-vortex state [5], are predicted. These four mechanisms can explain the paramagnetic limiting field being much higher than B_P^{BCS}. The helical-vortex-state mechanism cannot be applied to the present case because it is expected to work for $B \perp c$ [5].

Unlike the $B_{c2}(0)$ of $CeRhSi_3$ for $B \parallel a$ and other HF SCs, that for $B \parallel c$ is outstandingly high. Such a high $B_{c2}(0)$ and anisotropy are unlikely to be explained by a small and anisotropic g factor. The Wilson ratio $R_W = (\pi^2 k_B^2 \chi)/[g^2\mu_B^2 J(J+1)\gamma] = 2$ gives $g_a = 3.2$ and $g_c = 2.1$ for the $B \parallel a$ and c axes, respectively [21], where we use $J = 1/2$, $\gamma = 120$ mJ/mol K^2, and the magnetic susceptibility $\chi_a = 8.3 \times 10^{-3}$ emu/mol and $\chi_c = 3.8 \times 10^{-3}$ emu/mol [22]. These values are close to the value for free electrons and are not highly anisotropic. Explaining the high $B_{c2}(0)$ by the strong-coupling model would require that a huge Δ, more than 10 times as large as Δ in BCS, should be realized. Neither of these mechanisms is likely to be a major cause of our results.

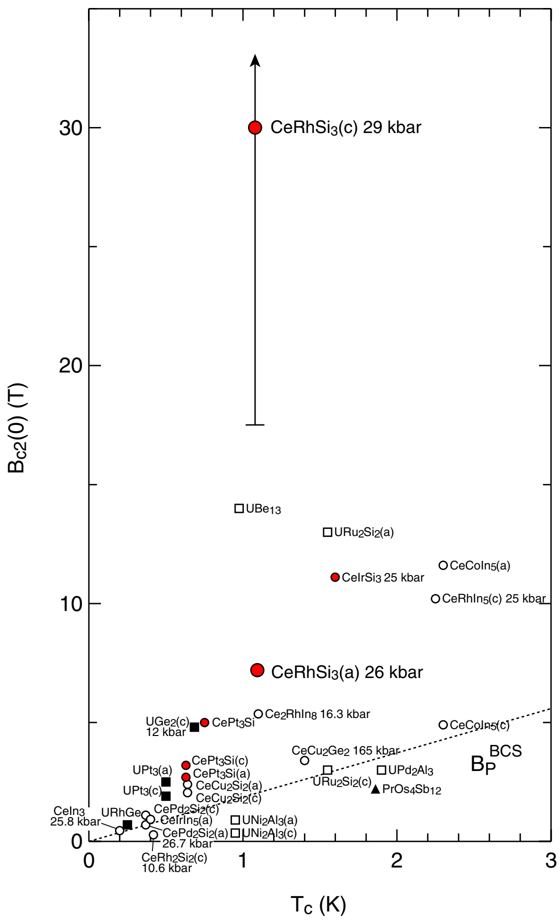

FIG. 3 (color online). Comparison of $B_{c2}(0)$ with B_P^{BCS} for HF (and related) SCs. The dotted line represents $B_P^{\mathrm{BCS}} = 1.86T_c$. The circles, squares, and triangle indicate cerium, uranium, and praseodymium compounds, respectively. The solid and hollow symbols mean (possibly) a triplet and singlet (or unclear) SCs, respectively. The gray (red online) marks denote a NCS SC. An a or c in parentheses denotes the applied field direction. The legends without parentheses indicate the results for single crystals for a cubic structure or for polycrystals. The plot of $CeRhSi_3$ for $B \parallel c$ indicates the estimated value. The up arrow indicates that $B_{c2}(0)$ of $CeRhSi_3$ for $B \parallel c$ should be larger than 17.5 T (see text).

According to the theory of the modified paramagnetic pair-breaking effect by Frigeri *et al.* [2,3], when the triplet component is predominant rather than the singlet one or when spin-orbit coupling is much larger than k_BT_c even in the singlet component, spin susceptibility does not change even in the superconducting state, so the paramagnetic pair-breaking effect is absent (or strongly reduced) for $B \parallel c$, while the paramagnetic effect is finite but greatly reduced for $B \parallel a$, as mentioned above. Our results of high $B_{c2}(0)$ (for $B \parallel c$) and its anisotropy evidently support this theory.

Even if the paramagnetic pair-breaking effect is absent, $B_{c2}(0)$ must be restricted by the orbital limiting field $B_{\rm orb}$. The $B_{c2}(0)$ of $CeRhSi_3$, however, obviously exceeds $B_{\rm orb}^{\rm BCS}$, as seen in the inset in Fig. 2(b). Moreover, the $B_{c2}(T)$ curve with positive curvature is quite different from the conventional BCS model [13]. Such phenomena are usually explained by the strong-coupling model [23].

We attempt to apply the strong-coupling model to $CeRhSi_3$. Note that the coupling is thought to be not the conventional electron-phonon type but the electron-magnon one. The dashed curves shown in the inset in Fig. 2(b) are reproduced from the prediction of the strong-coupling theory without the paramagnetic pair-breaking effect for a clean-limit SC [20]. The data at 15 ($T > 0.2T_c$) and 26 kbar ($T > 0.4T_c$) seem to correspond approximately to the curves for $\lambda = 10$ and 30, respectively. However, they deviate from the theoretical curves at low temperatures, and the data at 24 and 29 kbar do not trace the curve of any λ even near T_c.

The above consideration is based on the assumption of a spherical Fermi surface (FS). When the FS is distorted from a spherical one and approaches the Brillouin zone, the $B_{c2}(T)$ curve is modified, especially at low temperature [24]. Considering the complicated shapes of the FS in $CeRhSi_3$ [22], the FS may indeed approach the Brillouin zone. To reproduce the data more precisely, we must take into account a more realistic FS model in addition to the simple strong-coupling model. However, the effect of the modifications due to an anisotropic FS is unlikely to explain the P dependence of the $B_{c2}(T)$ curve. The disagreement between the simple strong-coupling model and the actual data differs for different pressures. The data for 15 kbar are above the curve of the strong-coupling model, while those for 26 kbar are below it. The temperature ranges of the deviations for different pressures are different. On the other hand, the FS changes continuously from 0 to 29.5 kbar [25]. We would expect the modifications by the anisotropic FS to change continuously with P. In addition, the extremely high value of $\lambda = 30$ is unlikely to be realistic in comparison with values for UGe_2 ($\lambda = 14$) [17] and UBe_{13} ($\lambda = 14.5$) [20]. We may have to take into account another effect, e.g., the broken inversion symmetry or a more complicated magnetic fluctuation, in addition to the present model.

In summary, we have observed an extremely high $B_{c2}(0)$ for $B \parallel c$ near the pressure that gives maximum T_c. $B_{c2}(0)$ exceeds both $B_P^{\rm BCS}$ and $B_{\rm orb}^{\rm BCS}$. The much higher $B_{c2}(0)$ than $B_P^{\rm BCS}$ for $B \parallel c$ and strong anisotropy of $B_{c2}(0)$ are consistent with the theory for NCS SCs, which predicts a reduced and anisotropic paramagnetic pair-breaking effect. On the other hand, the exceeding of $B_{\rm orb}^{\rm BCS}$ and the unusual shape of the $B_{c2}(T)$ curve cannot be explained satisfactorily by the strong-coupling model including modifications due to an anisotropic FS.

We thank M. Suzuki and M. Kikuchi for technical support. This work was supported by a Grant-in-Aid for Scientific Research from JSPS and partially by MEXT of Japan through a 21st Century COE Program "Exploring New Science by Bridging Particle-Matter Hierarchy."

[1] L. P. Gor'kov and E. I. Rashba, Phys. Rev. Lett. **87**, 037004 (2001).
[2] P. A. Frigeri, D. F. Agterberg, and M. Sigrist, New J. Phys. **6**, 115 (2004).
[3] P. A. Frigeri *et al.*, Phys. Rev. Lett. **92**, 097001 (2004); **93**, 099903(E) (2004).
[4] V. P. Mineev, Phys. Rev. B **71**, 012509 (2005).
[5] R. P. Kaur, D. F. Agterberg, and M. Sigrist, Phys. Rev. Lett. **94**, 137002 (2005).
[6] E. Bauer *et al.*, Phys. Rev. Lett. **92**, 027003 (2004).
[7] N. Kimura *et al.*, Phys. Rev. Lett. **95**, 247004 (2005).
[8] Y. Muro *et al.*, J. Phys. Soc. Jpn. **67**, 3601 (1998).
[9] K. Kadowaki and S. B. Woods, Solid State Commun. **58**, 507 (1986).
[10] In the ac-susceptibility measurements with a different magnet, we have confirmed the superconductivity up to at least 17.5 T for pressures from 23 to 29 kbar.
[11] W. Assmus *et al.*, Phys. Rev. Lett. **52**, 469 (1984).
[12] G. Knebel *et al.*, Phys. Rev. B **65**, 024425 (2001); M. Ohashi *et al.*, *ibid.* **68**, 144428 (2003); R. A. Fisher *et al.*, *ibid.* **65**, 224509 (2002); H. Shishido *et al.*, *ibid.* **66**, 214510 (2002); S. Araki *et al.*, J. Phys. Condens. Matter **14**, L377 (2002); H. Kotegawa *et al.*, J. Phys. Soc. Jpn. **75**, 044713 (2006).
[13] E. Helfand and N. R. Werthamer, Phys. Rev. **147**, 288 (1966).
[14] T. Yasuda *et al.*, J. Phys. Soc. Jpn. **73**, 1657 (2004).
[15] M. B. Maple *et al.*, in *The Physics of Superconductivity*, edited by K. H. Bennenman and J. B. Ketterson (Springer, Berlin, 2004), Vol. II, Sec. 8; I. Sugitani *et al.*, J. Phys. Soc. Jpn. **75**, 043703 (2006); T. Terashima *et al.*, Physica (Amsterdam) **378B–380B**, 991 (2006).
[16] J. P. Brison *et al.*, Physica (Amsterdam) **250C**, 128 (1995);
[17] I. Sheikin *et al.*, Phys. Rev. B **64**, 220503(R) (2001).
[18] B. S. Chandrasekhar, Appl. Phys. Lett. **1**, 7 (1962); A. M. Clogston, Phys. Rev. Lett. **9**, 266 (1962).
[19] C. F. Miclea *et al.*, Phys. Rev. Lett. **96**, 117001 (2006).
[20] F. Thomas *et al.*, J. Low Temp. Phys. **102**, 117 (1996).
[21] The magnetic susceptibility consists of the spin and Van Vleck parts. Strictly speaking, we must take account of the latter part. To explain $B_{c2}(0) = 30$ T, however, the Van Vleck part must be about 200 times as large as the spin one, which is unlikely to be realistic.
[22] N. Kimura *et al.*, Physica (Amsterdam) **294B–295B**, 280 (2001).
[23] L. N. Bulaevskii, O. V. Dolgov, and M. O. Ptitsyn, Phys. Rev. B **38**, 11 290 (1988).
[24] T. Kita and M. Arai, Phys. Rev. B **70**, 224522 (2004).
[25] T. Terashima *et al.* (to be published).